HHS Public Access

Author manuscript

Science. Author manuscript; available in PMC 2017 September 05.

Published in final edited form as:

Science. 2016 January 08; 351(6269): 186–190. doi:10.1126/science.aad0512.

Polysialylation controls dendritic cell trafficking by regulating chemokine recognition

Eva Kiermaier[1,*,§], **Christine Moussion**[1,*], **Christopher T. Veldkamp**[2,3], **Rita Gerardy-Schahn**[4], **Ingrid de Vries**[1], **Larry G. Williams**[2], **Gary R. Chaffee**[2], **Andrew J. Phillips**[2], **Friedrich Freiberger**[4], **Richard Imre**[5], **Deni Taleski**[6], **Richard J. Payne**[6], **Asolina Braun**[7], **Reinhold Förster**[8], **Karl Mechtler**[5], **Martina Mühlenhoff**[4], **Brian F. Volkman**[3], and **Michael Sixt**[1,§,*]

[1]Institute of Science and Technology Austria (IST Austria), am Campus 1, 3400 Klosterneuburg, Austria

[2]Department of Chemistry, University of Wisconsin-Whitewater, 800 West Main Street, Whitewater, Wisconsin 53190, United States

[3]Department of Biochemistry, Medical College of Wisconsin, 8701 Watertown Plank Road, Milwaukee, Wisconsin 53226, United States

[4]Institute for Cellular Chemistry, Hannover Medical School (MHH), Carl-Neuberg-Strasse 1, 30625 Hannover, Germany

[5]Research Institute of Molecular Pathology (IMP), Vienna Biocenter, Dr. Bohr Gasse 7, 1030 Vienna, Austria

[6]School of Chemistry, The University of Sydney, Sydney, New South Wales 2006, Australia

[7]Department of Microbiology and Immunology, The University of Melbourne at the Peter Doherty Institute for Infection and Immunity, Melbourne, Victoria 3000, Australia

[8]Institute of Immunology, Hannover Medical School (MHH), Carl-Neuberg-Strasse 1, 30625 Hannover, Germany

Abstract

The addition of polysialic acid to N- and/or O-linked glycans, referred to as polysialylation, is a rare posttranslational modification mainly known to control developmental plasticity of the nervous system. Here we show that CCR7, the central chemokine receptor controlling immune cell trafficking to secondary lymphatic organs, carries polysialic acid. This modification is essential for recognition of the CCR7 ligand CCL21. As a consequence, dendritic cell trafficking is abrogated in polysialyltransferase deficient mice, manifesting in disturbed lymph node homeostasis and unresponsiveness to inflammatory stimuli. Structure-function analysis of chemokine-receptor interactions reveals that CCL21 adopts an autoinhibited conformation, which is released upon

Correspondence to: Eva Kiermaier; eva.kiermaier@ist.ac.at, phone +43 2243 90003808. Michael Sixt; Sixt@ist.ac.at, phone +43 2243 90003801.

*contributed equally

interaction with polysialic acid. Thus, we describe a glycosylation-mediated immune cell trafficking disorder and its mechanistic basis.

Main Text

Polysialylation is a rare posttranslational modification executed by the two enzymes ST8Sia II and ST8Sia IV (1). These polysialyltransferases generate long α2,8-linked linear homopolymers of sialic acid, which are attached to N- and/or O-linked glycans (2). Polysialylation is mainly known to control developmental plasticity of the vertebrate nervous system via modulation of cell-cell and cell-matrix adhesions (3). Polysialic acid (polySia) further promotes cancer growth and metastasis via largely unknown mechanisms (4, 5) and, as such, is pursued as a therapeutic target (6). Recent evidence also suggests various functional implications during immune responses (7–10).

We immunologically characterized mice lacking ST8Sia IV (11), the polysialyltransferase expressed in hematopoietic cells. Under steady state conditions mutant animals showed severely reduced cellularity of peripheral lymph nodes (LNs) (Figure 1A), and frequently lacked small popliteal LNs (10 lymph nodes missing out of 16 analyzed). Infliction of inflammatory stimuli failed to trigger LN swelling compared to control animals (Figure 1B). In contrast, cellularity of the spleen was unaffected (Figure 1A), which might indicate specific defects in lymphocyte homing to LNs. However, we could not detect polySia on the surface of T and B cells and we did not observe any cell autonomous trafficking defects in the lymphocyte compartment (Figure S1A, B). In contrast, polySia was readily detectable on the surface of dendritic cells (DCs) during steady state (Figure 1C, upper panel and S1C) and it was additionally elevated upon inflammatory stimulation (Figure 1C, lower panel). LNs of *St8sia4*-deficient mice contained reduced amounts of DC subsets known to immigrate from peripheral tissues into the LN (Fig. 1D). Although DCs constitute only approximately 1% of cells in the LN they control LN size by instructing stromal cells to recruit lymphocytes and maintain their homeostasis (12, 13). Hence, a reduced size of the DC compartment might provide a potential explanation for reduced overall LN size. To test if defective immigration from the periphery was responsible for reduced DC numbers in LNs we performed skin-painting experiments, where endogenous DCs of the skin are mobilized and subsequently immigrate, via the afferent lymphatic vessels, into the draining LN (14). In *St8sia4*-deficient mice immigration of DCs into draining LNs was almost completely abrogated (Figure 1E).

We next used an in vitro reconstituted system to measure the migratory potential of polySia deficient DCs. To this end we generated DCs in vitro from bone marrow precursors. We confirmed that control cells up-regulate polySia upon inflammatory stimulation, while *St8sia4*-deficient cells differentiated normally but completely lacked polySia (Figure S1D. When we co-injected control and *St8sia4*-deficient DCs into footpads of wildtype recipient mice polySia-deficient DCs were completely unable to enter LNs (Figure 2A), formally showing that polySia-dependency is cell-autonomous. We next incorporated the in vitro generated DCs into 3D collagen gels and exposed them to gradients of the chemokines CCL19 and CCL21 (Figure 2B). By binding to CCR7 these chemokines are required to

guide DCs into the draining LN (15). While the migratory response towards gradients of CCL19 was equally efficient for control and knockout cells, polySia-deficient DCs were completely refractory to CCL21 (Figure 2B). Similarly, signaling, as measured by Akt and Erk phosphorylation, was largely abolished in response to CCL21, while the CCL19 triggered signal was comparable to control cells (Figure S2). Hence, polySia-deficient DCs were capable of differentiating and migrating regularly but were selectively unresponsive towards CCL21.

En route from the periphery into the LN CCL21 mediates two key steps: i) directed interstitial migration towards the dermal lymphatic vessel and ii) migration from the LN's subcapsular sinus into the deep T cell area. To exclude any confounding effects of CCL19 we probed DC migration in *Ccl19*-deficient hosts. To bypass the skin and directly measure migration within the LN we injected DCs into the afferent lymphatic vessel(16) (Figure S3A). Within the LN, polySia-deficient DCs behaved like control cells and entered the deep T cell parenchyma, while *Ccr7*-deficient DCs were unable to leave the subcapsular sinus, as previously shown (Figure 2C (16) Next, we selectively probed migration within the skin and co-incubated skin explants with polySia-deficient and control DCs. We found that only control cells entered the dermal lymphatic vessels, while polySia-deficient DCs did not even infiltrate the dermal interstitium (Figure 2D), therefore precisely phenocopying *Ccr7*-deficient DCs(17). Similarly, when culturing ear-explants of *St8sia4*-deficient mice, DCs remained in the interstitium and failed to enter the lumen of lymphatic vessels as seen in control tissue (Figure S3B). Hence, DCs require polySia to sense "dermal CCL21", while sensing of "LN CCL21" is polySia independent. Tissue-context specific presentation of CCL21 might explain why T cells, which do not express polySia are able to home into LNs of *Ccl19*-deficient mice (18), although they only responded to CCL19 but not to CCL21, when exposed to soluble chemokine (Figure S3C). This prompted us to study the molecular mechanism underlying polySia-dependent CCL21 sensing.

While the chemokine domain of CCL21 is structurally similar to CCL19 (19, 20), CCL21 carries a positively charged C-terminal extension which mediates binding to glycans, in particular heparan sulfate residues (21). It was suggested that, via these residues, CCL21 might also interact with negatively charged polySia (9). Consequently, cell surface polySia might act as a co-receptor and increase the local availability of CCL21 for CCR7 (22). Of the seven proteins that were described as polySia carriers (2), only neuropilin-2 was expressed on mature DCs (7, 23). However, in vivo and in vitro migration assays with neuropilin-2 deficient DCs did not show any perturbed migratory responses (Figure S4A, B). As neuropilin-2 deficient DCs still carried polySia, we immunoprecipitated polySia from lysates of mature DCs and used mass spectrometry to identify the underlying protein scaffold(s). This unbiased approach revealed three previously unknown putative polySia carriers, including CCR7 (Figure S4C and table S1). CCR7 and neuropilin-2 emerged as the only candidate molecules exposed on the cell surface.

This suggests that, apart from neuropilin-2, CCR7 is a second polySia carrier on the surface of mature DCs. To follow up CCR7 as a direct target of polysialylation we employed a HEK293 cell system. When GFP was immunoprecipitated from lysates of cells co-expressing a CCR7-GFP fusion protein and ST8Sia IV, polySia could be detected in the

precipitate, while it was absent in precipitates of both single transfectants (Figure 3A). Vice versa, precipitation of polySia revealed CCR7-GFP specifically in the double transfectants (Figure 3B). Further biochemical and mutational analysis in HEK293 cells indicated that polySia was attached to both N- and O-linked glycans of CCR7 since inhibition of either N- or O-glycosylation did not fully abrogate polysialylation of CCR7 (Figure S4D and S4E). To substantiate that CCR7 is polysialylated in DCs, we used flow cytometry to analyze cell surface levels of polySia in CCR7-deficient and control DCs and found reduced polySia on CCR7-deficient cells (Figure 3C). This suggests that, apart from neuropilin-2, CCR7 is a second carrier of polySia on the surface of mature DCs.

A co-receptor model would predict that polySia on CCR7 might bind CCL21's C-terminus, thereby effectively increasing receptor to ligand affinity. To test this idea we C-terminally truncated CCL21 and performed chemotaxis assays. At odds with a co-receptor model, the responsiveness of polySia-deficient DCs to CCL21 was restored when the chemokine was C-terminally truncated (Figure 4A). This finding indicated that rather than enhancing CCR7 binding to CCL21, the polySia-CCL21 interaction might promote signaling by releasing CCL21 from an otherwise inactive state. This would be consistent with an autoinhibition model, in which the C-terminus of CCL21 induces structural alterations within the chemokine domain that prevent signaling but can be reversed upon polySia binding.

Notably, CCL21's C-terminus is unstructured and does not adopt a stable fold (20). We therefore performed NMR spectroscopy to detect chemical shifts that might distinguish the chemokine domain conformation of full length from that of C-terminally truncated CCL21. As expected, truncation caused chemical shift changes in residues with immediate proximity to the truncation site (Figure S5A). However, additional chemical shifts localized to the α-helix of the chemokine domain (residues 63, 64, 66, 67, 69 and 70) and to additional residues (26, 31, 41, 47 and 54; Figure 4B and S5A). These shift perturbations distal to the site of truncation suggest that CCL21's C-terminus transiently interacts with the chemokine domain of CCL21, thereby providing a putative structural correlate of functional autoinhibition. When polySia was titrated to full length CCL21, residues belonging to the putative autoinhibition signature shifted to similar positions as observed in the spectra of truncated CCL21 (Figure 4C and S5B). Hence, in the presence of polySia the chemokine domain of full length CCL21 adopts a similar conformation as in C-terminally truncated CCL21. PolySia binding to truncated CCL21 was considerably weaker compared to full length CCL21, confirming interactions mainly via the C-terminus (Figure S5C). Together, these data suggest that CCL21's C-terminus structurally alters CCL21's chemokine domain most likely by transient binding and that this structural alteration is abrogated by polySia binding to CCL21's C-terminal extension.

To functionally challenge the autoinhibition model, we took advantage of the fact that the polySia-insensitive chemokine CCL19 naturally lacks a C-terminal extension and produced a recombinant chemokine with CCL21's C-terminus transplanted to CCL19 (Figure 4D, right panel). Chemotaxis assays revealed that control DCs responded to the chimeric chemokine with kinetics that were more similar to CCL21 than to CCL19 (Figure 4D, left panel). The maximal directed response of wild type DCs towards the chimera was slightly diminished in comparison to CCL19. Most relevant, transplantation of CCL21's C-terminus

to CCL19 conferred polySia-sensitivity since the response of polySia-deficient DCs to the chimeric chemokine was largely abrogated. These data corroborate a model in which polySia releases CCL21 from an autoinhibited state by interacting with CCL21's C-terminus.

In summary, we describe a glycosylation-dependent immune cell trafficking defect and its underlying molecular mode of action. PolySia-dependent release of CCL21 autoinhibition is a mechanism of chemokine regulation that is likely to be relevant for other chemokines containing similar C-terminal extensions. The finding that polySia dependency is restricted to the skin, suggests that, depending on the molecular context, CCL21 can either be presented in the auto-inhibited or the active form. The mechanism we describe also illuminates how glycosylation of a G-protein coupled receptor allows discrimination between two alternative ligands. Apart from being the key-coordinator of adaptive immune cell trafficking, the CCR7-axis is also centrally involved in metastatic tumor spread, suggesting potential therapeutic relevance of our findings.

Supplementary Material

Refer to Web version on PubMed Central for supplementary material.

Acknowledgments

We thank S. Schüchner and E. Ogris for kindly providing the α-GFP antibody, M. Helmbrecht and A. Huber for providing *Nrp-2*−/− mice and the IST Scientific Support Facilities for excellent services. We thank J. Renkawitz and K. Vaahtomeri for critically reading the manuscript. The data described in this manuscript are tabulated in the main paper and in the supplementary materials. This work was supported by the European Research Council (ERC GA 281556 to M.S. and ERC GA 322645 to R.F.), the EU FP7 ITN STROMA and a START Award of the Austrian Science Foundation (FWF) to M.S. and the National Institute of Health (NIH grant 1R15CA159202-01 to C.T.V and NIH grants R01AI058072 and R01GM09738 to B.F.V).

References

1. Rutishauser U. Polysialic acid in the plasticity of the developing and adult vertebrate nervous system. Nat Rev Neurosci. 2008; 9:26–35. [PubMed: 18059411]
2. Mühlenhoff M, Rollenhagen M, Werneburg S, Gerardy-Schahn R, Hildebrandt H. Polysialic acid: versatile modification of NCAM, SynCAM 1 and neuropilin-2. Neurochem Res. 2013; 38:1134–1143. [PubMed: 23354723]
3. Schnaar RL, Gerardy-Schahn R, Hildebrandt H. Sialic acids in the brain: gangliosides and polysialic acid in nervous system development, stability, disease, and regeneration. Physiological Reviews. 2014; 94:461–518. [PubMed: 24692354]
4. Falconer RA, Errington RJ, Shnyder SD, Smith PJ, Patterson LH. Polysialyltransferase: a new target in metastatic cancer. Curr Cancer Drug Targets. 2012; 12:925–939. [PubMed: 22463390]
5. Harduin-Lepers A, et al. Sialyltransferases functions in cancers. Front Biosci (Elite Ed). 2012; 4:499–515. [PubMed: 22201891]
6. Al-Saraireh YMJ, et al. Pharmacological Inhibition of polysialyltransferase ST8SiaII Modulates Tumour Cell Migration. PLoS ONE. 2013; 8:e73366. [PubMed: 23951351]
7. Curreli S, Arany Z, Gerardy-Schahn R, Mann D, Stamatos NM. Polysialylated neuropilin-2 is expressed on the surface of human dendritic cells and modulates dendritic cell-T lymphocyte interactions. J Biol Chem. 2007; 282:30346–30356. [PubMed: 17699524]
8. Rey-Gallardo A, et al. Polysialylated neuropilin-2 enhances human dendritic cell migration through the basic C-terminal region of CCL21. Glycobiology. 2010; 20:1139–1146. [PubMed: 20488940]

9. Bax M, van Vliet SJ, Litjens M, García-Vallejo JJ, van Kooyk Y. Interaction of polysialic acid with CCL21 regulates the migratory capacity of human dendritic cells. PLoS ONE. 2009; 4:e6987. [PubMed: 19750015]
10. Drake PM, et al. Polysialic acid, a glycan with highly restricted expression, is found on human and murine leukocytes and modulates immune responses. The Journal of Immunology. 2008; 181:6850–6858. [PubMed: 18981104]
11. Eckhardt M, et al. Mice deficient in the polysialyltransferase ST8SiaIV/PST-1 allow discrimination of the roles of neural cell adhesion molecule protein and polysialic acid in neural development and synaptic plasticity. J Neurosci. 2000; 20:5234–5244. [PubMed: 10884307]
12. Moussion C, Girard JP. Dendritic cells control lymphocyte entry to lymph nodes through high endothelial venules. Nature. 2011; 479:542–546. [PubMed: 22080953]
13. Wendland M, et al. Lymph Node T Cell Homeostasis Relies on Steady State Homing of Dendritic Cells. Immunity. 2011; 35:945–957. [PubMed: 22195748]
14. Macatonia SE, Knight SC, Edwards AJ, Griffiths S, Fryer P. Localization of antigen on lymph node dendritic cells after exposure to the contact sensitizer fluorescein isothiocyanate. Functional and morphological studies. J Exp Med. 1987; 166:1654–1667. [PubMed: 3119761]
15. Forster R, et al. CCR7 coordinates the primary immune response by establishing functional microenvironments in secondary lymphoid organs. Cell. 1999; 99:23–33. [PubMed: 10520991]
16. Braun A, et al. Afferent lymph–derived T cells and DCs use different chemokine receptor CCR7–dependent routes for entry into the lymph node and intranodal migration. Nat Immunol. 2011; 12:879–887. [PubMed: 21841786]
17. Weber M, et al. Interstitial Dendritic Cell Guidance by Haptotactic Chemokine Gradients. Science. 2013; 339:328–332. [PubMed: 23329049]
18. Link A, et al. Fibroblastic reticular cells in lymph nodes regulate the homeostasis of naive T cells. Nat Immunol. 2007; 8:1255–1265. [PubMed: 17893676]
19. Veldkamp CT, et al. Solution Structure of CCL19 and Identification of Overlapping CCR7 and PSGL-1 Binding Sites. Biochemistry. 2015; 54:4163–4166. [PubMed: 26115234]
20. Love M, et al. Solution Structure of CCL21 and Identification of a Putative CCR7 Binding Site. Biochemistry. 2012; 51:733–735. [PubMed: 22221265]
21. Hirose J. Versican Interacts with Chemokines and Modulates Cellular Responses. Journal of Biological Chemistry. 2000; 276:5228–5234. [PubMed: 11083865]
22. Rey-Gallardo A, Delgado-Martin C, Gerardy-Schahn R, Rodriguez-Fernandez JL, Vega MA. Polysialic acid is required for neuropilin-2a/b-mediated control of CCL21-driven chemotaxis of mature dendritic cells and for their migration in vivo. Glycobiology. 2011; 21:655–662. [PubMed: 21199821]
23. Rollenhagen M, et al. Polysialic acid on neuropilin-2 Is exclusively synthesized by the polysialyltransferase ST8SiaIV and attached to mucin-type O-glycans located between b2 and c domain. Journal of Biological Chemistry. 2013; doi: 10.1074/jbc.M113.463927
24. Frosch M, Görgen I, Boulnois GJ, Timmis KN, Bitter-Suermann D. NZB mouse system for production of monoclonal antibodies to weak bacterial antigens: isolation of an IgG antibody to the polysaccharide capsules of Escherichia coli K1 and group B meningococci. Proc Natl Acad Sci USA. 1985; 82:1194–1198. [PubMed: 3919387]
25. Jokilammi A, et al. Construction of antibody mimics from a noncatalytic enzyme-detection of polysialic acid. 2004; 295:149–160.
26. Schwarzer D, et al. Proteolytic release of the intramolecular chaperone domain confers processivity to endosialidase F. J Biol Chem. 2009; 284:9465–9474. [PubMed: 19189967]
27. Lu Q, et al. Optimized procedures for producing biologically active chemokines. Protein Expr Purif. 2009; 65:251–260. [PubMed: 19297698]
28. Lutz MB, et al. An advanced culture method for generating large quantities of highly pure dendritic cells from mouse bone marrow. 1999; 223:77–92.
29. Ammermann TL, et al. Rapid leukocyte migration by integrin-independent flowing and squeezing. Nature. 2008; 453:51–55. [PubMed: 18451854]

30. Windfuhr M, Manegold A, Muhlenhoff M, Eckhardt M, Gerardy-Schahn R. Molecular defects that cause loss of polysialic acid in the complementation group 2A10. J Biol Chem. 2000; 275:32861–32870. [PubMed: 10921918]

31. Tan JHY, et al. Tyrosine Sulfation of Chemokine Receptor CCR2 Enhances Interactions with Both Monomeric and Dimeric Forms of the Chemokine Monocyte Chemoattractant Protein-1 (MCP-1). 2013; 288:10024–10034.

32. Keys TG, et al. Engineering the product profile of a polysialyltransferase. 2014; 10:437–442.

33. Riol-Blanco L, et al. The chemokine receptor CCR7 activates in dendritic cells two signaling modules that independently regulate chemotaxis and migratory speed. J Immunol. 2005; 174:4070–4080. [PubMed: 15778365]

34. Walz A, Rodriguez I, Mombaerts P. Aberrant sensory innervation of the olfactory bulb in neuropilin-2 mutant mice. Journal of Neuroscience. 2002; 22:4025–4035. [PubMed: 12019322]

35. Schaeuble K, et al. Ubiquitylation of the chemokine receptor CCR7 enables efficient receptor recycling and cell migration. Journal of Cell Science. 2012; 125:4463–4474. [PubMed: 22797918]

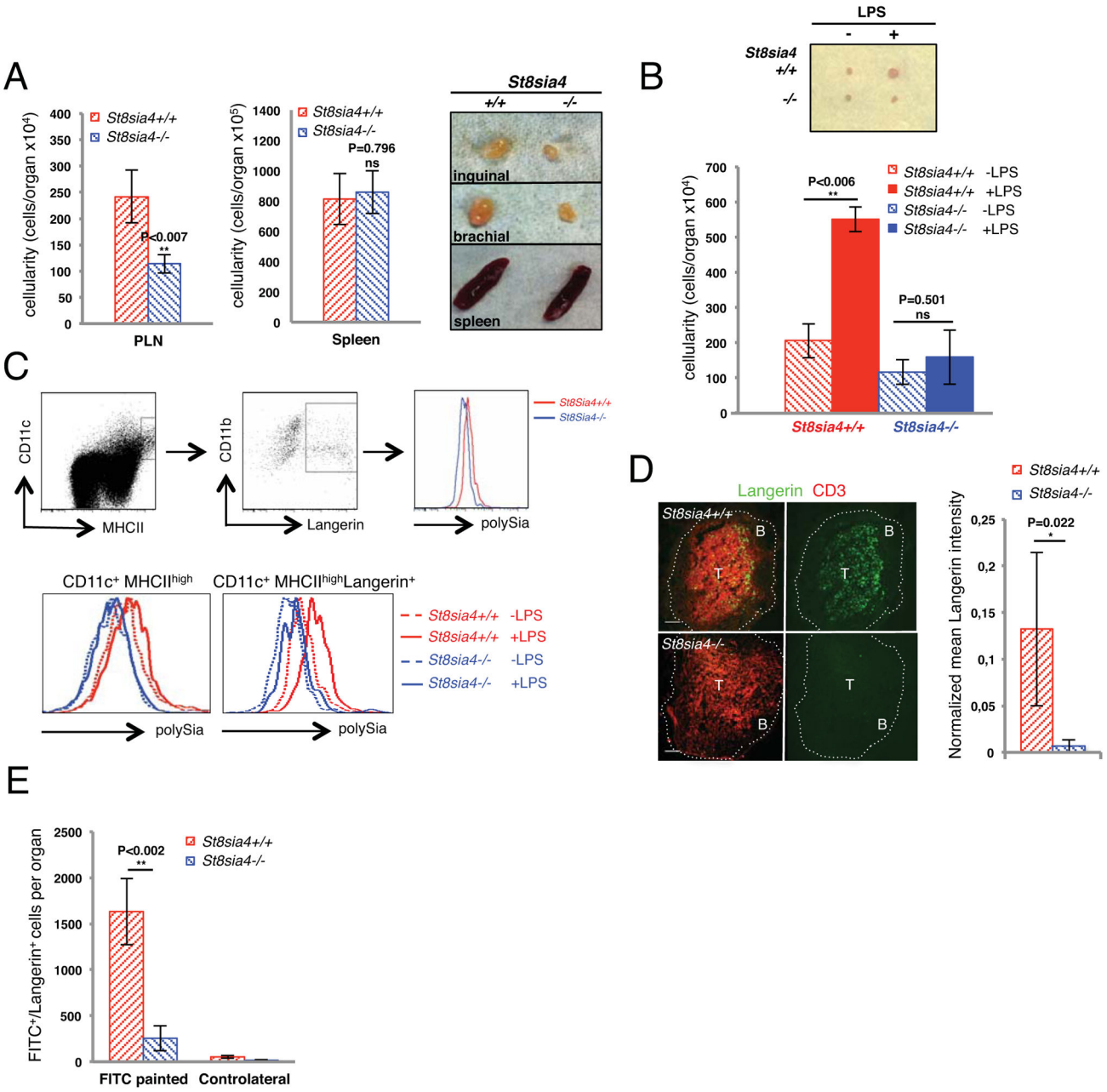

Fig. 1. PolySia on dendritic cells is required for regular lymph node homeostasis and regulates inflammatory responses

(A) (left) Cellularity of secondary lymphoid organs in *St8sia4−/−* and control mice. Graphs display total leukocyte numbers of single organs. Brachial and inguinal LNs have been pooled as peripheral LNs (PLN). Results are depicted as averages of three independent experiments of six different age-matched mice per genotype ±SD. Differences between the two groups were examined by two-tailed unpaired student's t-test. (right) Representative image of SLOs from *St8sia4−/−* and control mice. **(B)** LPS or PBS only (-LPS) were injected into the hind footpads of *St8sia4−/−* and control mice and popliteal LNs were analyzed 48 hours post-injection. Graph depicts average cellularity ±SD of three

independent experiments of seven animals analyzed per genotype. Differences between the two groups were examined by two-tailed unpaired student's t-test. **(C)** Flow cytometry of polySia levels on leukocytes isolated from popliteal LNs from *St8sia4−/−* and control mice in steady state (upper panel) and after LPS injection (lower panel). Migratory DCs are defined as $CD11c^{+}$ $MHCII^{high}$ and further classified by Langerin staining. **(D)** (left) Immunohistology of inguinal LNs from *St8sia4−/−* and control mice. B and T cell areas are indicated. Scale bar: 150μm. (right) Quantification of Langerin intensities. Bars represent normalized mean Langerin intensities ±SD of PLNs of three different mice per genotype. Differences between the two groups were examined by two-tailed unpaired student's t-test. **(E)** FITC painting of *St8sia4−/−* and control mice. Graph depicts average values ±SD of total numbers of $FITC^{+}$/$Langerin^{+}$ cells per organ of five different mice per genotype. Controls are derived from non-painted ears (controlateral). Differences between the two groups were examined by two-tailed unpaired student's t-test.

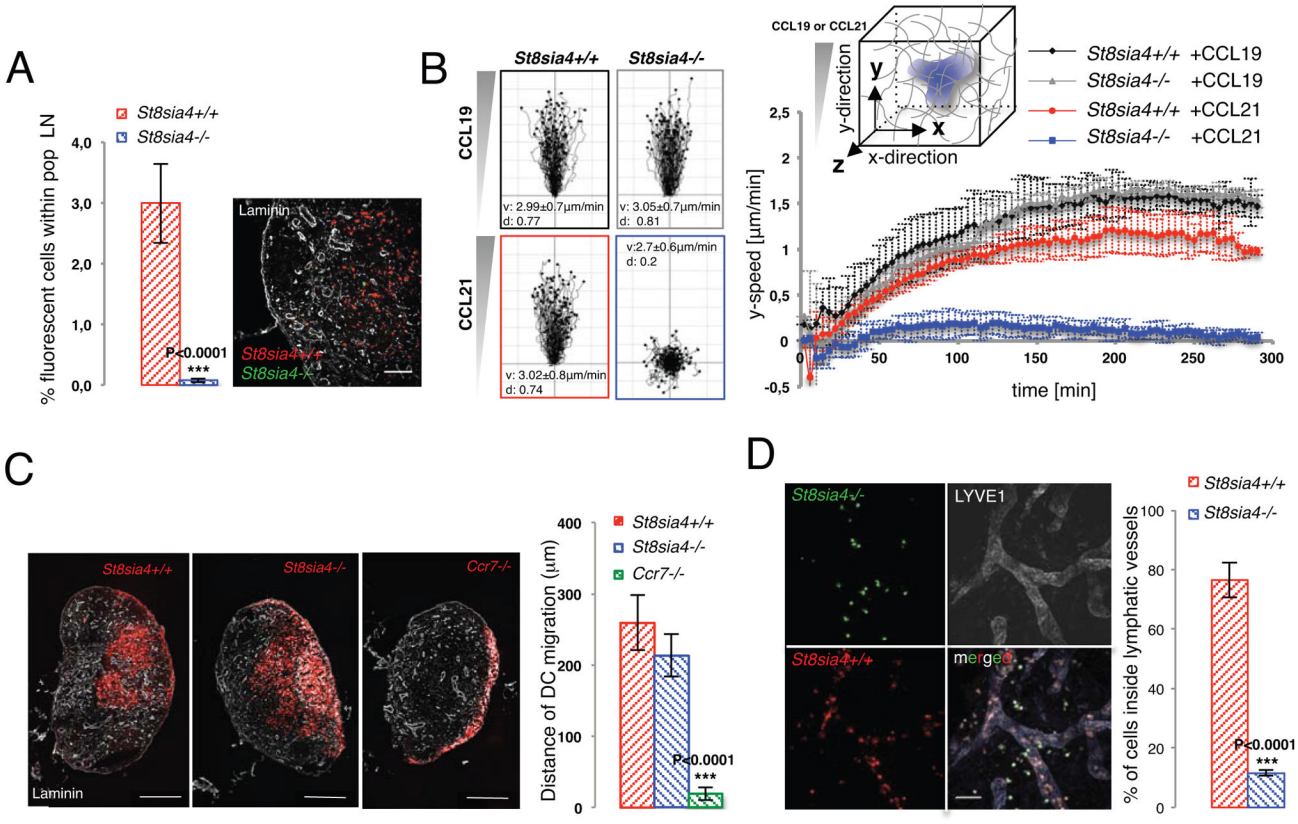

Fig. 2. PolySia affects CCL21 sensing in peripheral tissues

(A) Footpad injection of TAMRA- and CFSE-labeled *St8sia4−/−* and control BMDCs into wildtype recipient mice. Mice were sacrificed 48 hours post-injection and analyzed by flow cytometry (left) and immunohistochemistry (right). Cryosections of popliteal LNs were stained against laminin. Differences between the two groups were examined by two-tailed unpaired student's t-test. Scale bar: 100µm. **(B)** (left) Single cell tracks of *St8sia4−/−* and control BMDCs migrating within 3D collagen matrices towards CCL19 and CCL21 gradients (0.33µM/gel). Average velocities ±SD and directionality are indicated for each genotype and condition. (right) Automated analysis of y-directed velocities of DC migration in 3D collagen gels. Graphs depict average speed in y-direction ±SD over time of eight independent experiments with cells isolated from at least three different mice. **(C)** Intralymphatic injection of TAMRA-labeled *St8sia4−/−*, control or *Ccr7−/−* BMDCs into *Ccl19−/−* recipient mice. 10 hours post injection popliteal LNs were stained against laminin to visualize LN architecture (parenchyma and cortical sinus). Graph depicts average migratory distance ±SD of TAMRA$^+$ DCs from the LN edge to parenchyma (at least five mice per group). Differences between the two groups were examined by two-tailed paired student's t-test. Scale bar: 250 µm. **(D)** (left) z-stack projection of wildtype ear sheets incubated with *St8sia4−/−* and control BMDCs and stained against LYVE1. (right) Quantification of cells inside lymphatic vessels. Bars indicate average values ±SD of five different fields per view of three independent experiments. Differences between the two groups were examined by two-tailed unpaired student's t-test. Scale bar: 100µm.

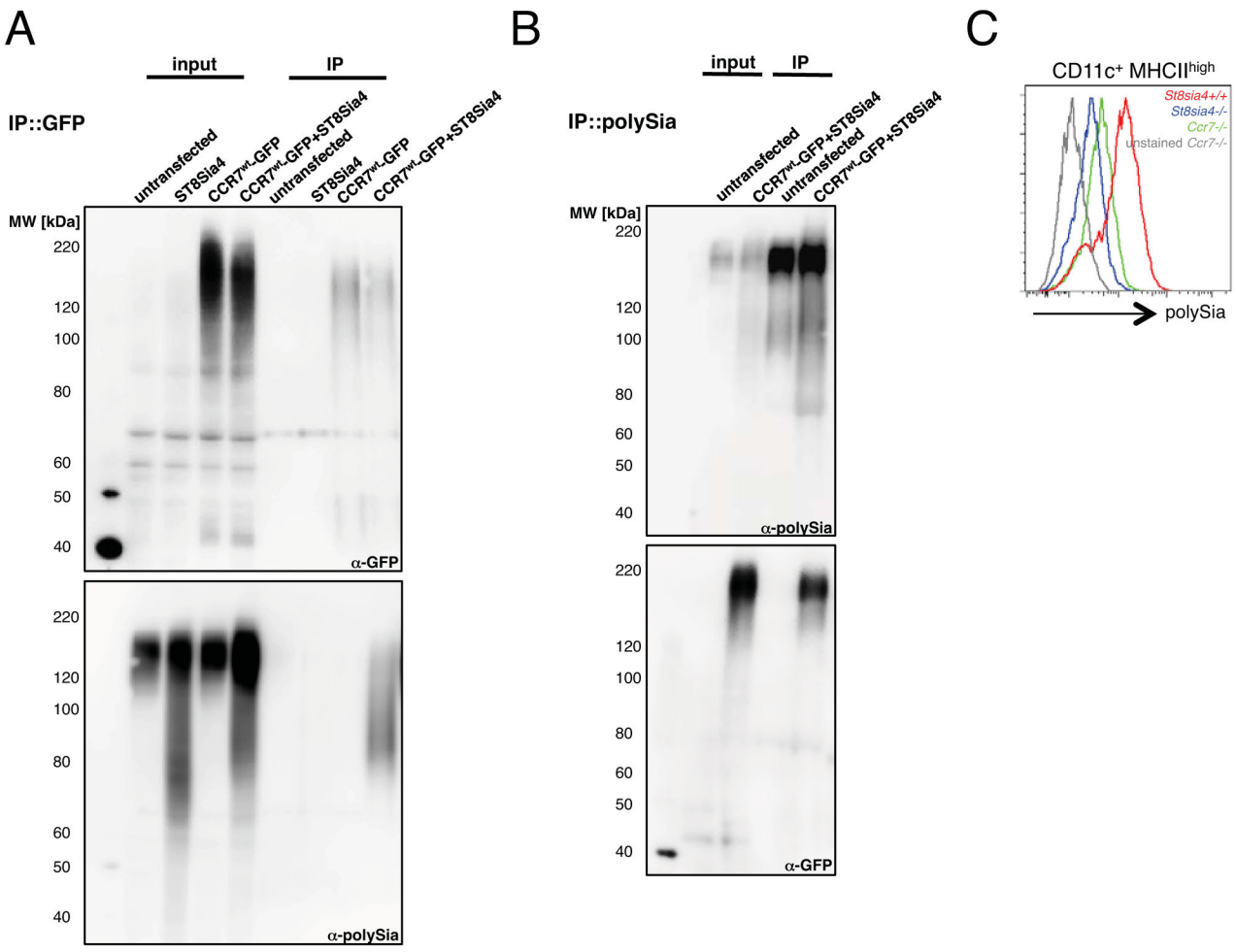

Fig. 3. CCR7 is polysialylated on mature dendritic cells

(A) Pull down of CCR7-GFP from HEK293 cells co-transfected with murine *Ccr7-gfp* and *St8sia4* plasmids. CCR7-GFP was immunoprecipitated with α-GFP-coupled magnetic beads (upper panel) and polySia detected with monoclonal antibody 735 (lower panel). Input represents 1/10 of total cell lysate. **(B)** Pull down of polysialylated proteins from HEK293 cells co-transfected with murine *Ccr7-gfp* and *St8sia4* plasmids. Polysialylated proteins were immunoprecipitated with iEndoN-coupled magnetic beads (upper panel) and CCR7-GFP detected using α-GFP antibody (lower panel). Input represents 1/10 of total cell lysate. **(C)** Flow cytometry of polySia cell surface levels on mature CD11c^{+} MHCII^{high} BMDCs.

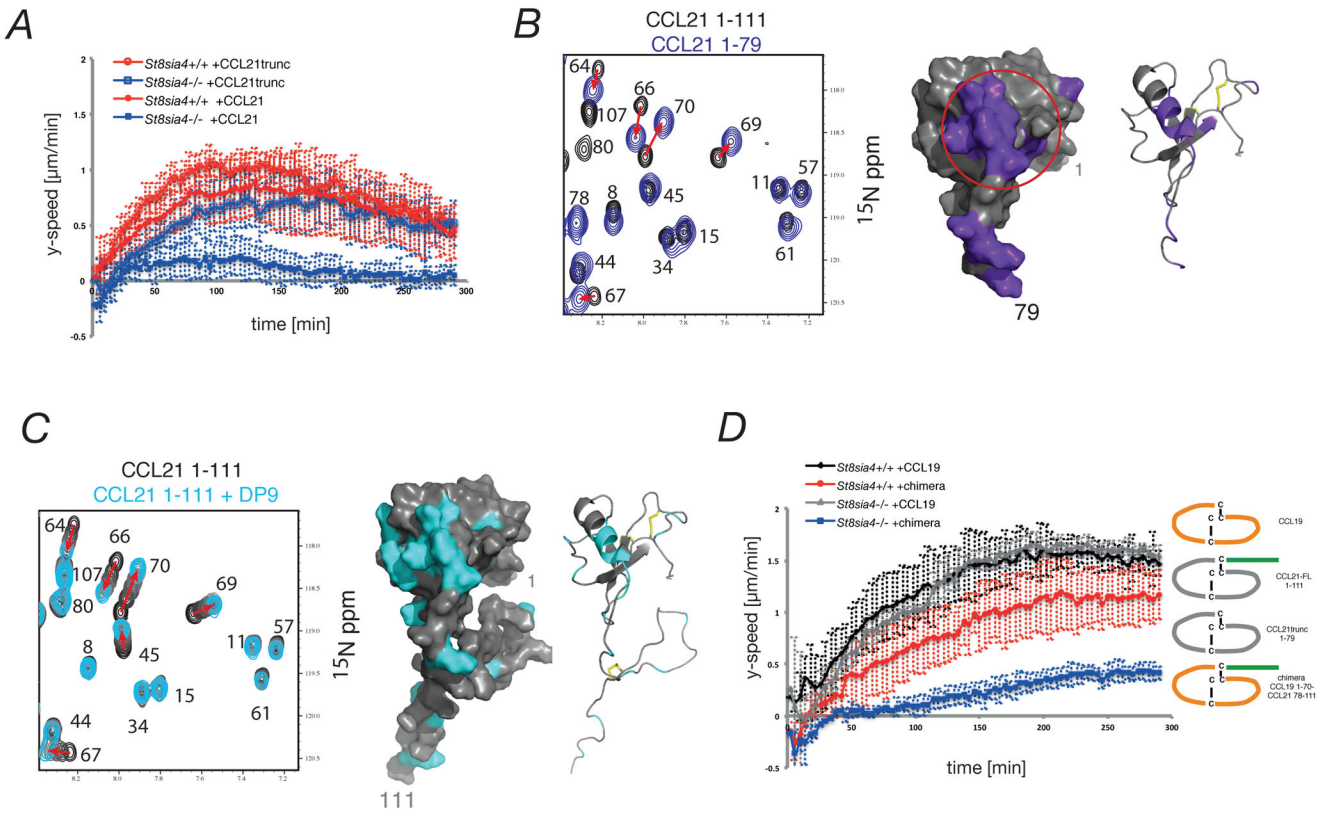

Fig. 4. Identification of an autoinhibitory interaction site within CCL21

(A) Migration of mature BMDCs within 3D collagen gels towards truncated CCL21 (CCL21trunc). All graphs depict average speed in y-direction ±SD over time of 8 independent experiments with cells generated from at least three different mice. **(B)** (left) Overlays of a portion of the ^{15}N-^{1}H HSQC spectra of CCL21-FL 1–111 (black) and CCL21trunc 1–79 (purple). (right) The first 79 amino acids of the CCL21-FL structure are depicted with residues showing significant changes in chemical shift perturbations upon truncation. Red circle indicates putative autoinhibitory site. **(C)** (left) Overlays of a portion of the ^{15}N-^{1}H HSQC spectra of CCL21-FL 1–111 (black) and CCL21-FL titrated with increasing concentrations of polySia DP9 (grays to cyan). (right) Residues within CCL21-FL with significant polySia induced chemical shift perturbations are colored cyan. **(D)** (right) Schematic representation of chemokines used for *in vitro* migration assays. FL: full length. (left) Migration of mature BMDCs towards the chimeric chemokine.